Am J Physiol Endocrinol Metab 305: E1230–E1240, 2013.
First published September 3, 2013; doi:10.1152/ajpendo.00081.2013.

Mouse and human islets survive and function after coating by biosilicification

David B. Jaroch,[1,5]* Jing Lu,[2,5]* Rajtarun Madangopal,[1,5] Natalie D. Stull,[6,7,8,9] Matthew Stensberg,[2,5] Jin Shi,[1,5] Jennifer L. Kahn,[2,5] Ruth Herrera-Perez,[2,5] Michael Zeitchek,[2,5] Jennifer Sturgis,[4] J. Paul Robinson,[4] Mervin C. Yoder,[7,8] D. Marshall Porterfield,[1,2,3,5] Raghavendra G. Mirmira,[6,7,8,9] and Jenna L. Rickus[1,2,5]

[1]*Weldon School of Biomedical Engineering, Purdue University, West Lafayette, Indiana;* [2]*Department of Agricultural and Biological Engineering, Purdue University, West Lafayette, Indiana;* [3]*Department of Horticulture and Landscape Architecture, Purdue University, West Lafayette, Indiana;* [4]*Purdue University Cytometry Laboratories, Purdue University, West Lafayette, Indiana;* [5]*Physiological Sensing Facility at the Bindley Bioscience Center and the Birck Nanotechnology Center, Purdue University, West Lafayette, Indiana;* [6]*Department of Medicine, Indiana University School of Medicine, Indianapolis, Indiana;* [7]*Herman B. Wells Center for Pediatric Research, Indiana University School of Medicine, Indianapolis, Indiana;* [8]*Department of Pediatrics, Indiana University School of Medicine, Indianapolis, Indiana; and* [9]*Department of Cellular and Integrative Physiology, Indiana University School of Medicine, Indianapolis, Indiana*

Submitted 12 February 2013; accepted in final form 27 August 2013

Jaroch DB, Lu J, Madangopal R, Stull ND, Stensberg M, Shi J, Kahn JL, Herrera-Perez R, Zeitchek M, Sturgis J, Robinson JP, Yoder MC, Porterfield DM, Mirmira RG, Rickus JL. Mouse and human islets survive and function after coating by biosilicification. *Am J Physiol Endocrinol Metab* 305: E1230–E1240, 2013. First published September 3, 2013; doi:10.1152/ajpendo.00081.2013.— Inorganic materials have properties that can be advantageous in bioencapsulation for cell transplantation. Our aim was to engineer a hybrid inorganic/soft tissue construct by inducing pancreatic islets to grow an inorganic shell. We created pancreatic islets surrounded by porous silica, which has potential application in the immunoprotection of islets in transplantation therapies for type 1 diabetes. The new method takes advantage of the islet capsule surface as a template for silica formation. Mouse and human islets were exposed to medium containing saturating silicic acid levels for 9–15 min. The resulting tissue constructs were then cultured for up to 4 wk under normal conditions. Scanning electron microscopy and energy dispersive X-ray spectroscopy was used to monitor the morphology and elemental composition of the material at the islet surface. A cytokine assay was used to assess biocompatibility with macrophages. Islet survival and function were assessed by confocal microscopy, glucose-stimulated insulin release assays, oxygen flux at the islet surface, expression of key genes by RT-PCR, and syngeneic transplant into diabetic mice.

islet; encapsulation; silica; coating; tissue engineering

TO CREATE 3D TISSUE CONSTRUCTS for transplantation therapies, cells are typically encapsulated within organic polymers, either synthetic or natural, such as collagen or alginate. For applications requiring protection from the immune system, however, inorganic or hybrid (inorganic/organic) materials may offer a different set of useful functions and properties to be used as alternatives to or in conjunction with the organic polymers. Porous silica is an attractive material for these applications because of its mesoporosity, potential to create hierarchical structures, optical transparency, capacity for biofunctionalization, performance in precision size exclusion, and bioactivity.

Our work focuses on primary pancreatic islets because of their importance in therapies for type 1 diabetes. The Edmonton protocol of islet transplantation in humans (40) has demonstrated remarkable short-term success, with 80% of individuals achieving insulin independence at 1 yr posttransplant; however, this rate decreases to only about 10–15% at 5 yr (3). Multiple mechanisms contribute to the progressive loss of graft function but likely include an immediate blood-mediated response (IBMR) (1, 37), poor revascularization and hypoxia (9, 16), and ongoing auto- and alloimmune responses (38). Protection of islets or stem cell-derived pseudo-islets by protective membranes could significantly improve transplant outcomes for patients.

The sol-gel synthesis method of forming solid porous silica under biologically friendly temperatures and pH has been used to encapsulate first biomolecules and later living cells since the early 1990s. Early attempts to use silica as a microencapsulation matrix for islets employed bulk sol-gel techniques, resulting in islets encased in thick silica slabs or spheres (34, 35). These implants were able to supply enough insulin to prevent urinary excretion of glucose in NOD mice for almost 11 wk (35); however, bulk materials can create issues by creating diffusion barriers, increasing hypoxia, increasing transplant volume, and inserting delays in the glucose-insulin control system. Carturan and colleagues achieved thin silica encapsulation of islets by using the Biosil process (5, 33). This method involves exposing cells to a gas stream comprised of N_2 and vaporized TEOS [$Si(OCH_2CH_3)_4$] and DEMS [$HSiCH_3(OCH_2CH_3)_2$]. Moisture in the atmosphere and on the cell surface allows for the reaction of the alkoxysilanes and deposition of a sol-gel shell. When implanted, the direct sol-gel silica tissue interface did not demonstrate signs of inflammatory cell aggregation or an immune reaction, providing evidence for the biocompatibility of the material used in tissue encapsulation applications (5).

Here, we present a process by which the islet surface acts as a nucleation site to template the formation of a thin, islet-specific, porous silica shell around primary murine and human islets in a liquid-medium environment. In essence, the islets grow their own protective shell. This simple, wet chemical process is conducted in growth medium under standard cell culture conditions, is amenable to a variety of methods for controlling physical, chemical, and biological material properties, and could easily be integrated into existing GMP islet

* D. B. Jaroch and J. Lu contributed equally to the publication.

Address for reprint requests and other correspondence: J. L. Rickus, 225 S. Univ. St., Purdue University, West Lafayette, IN 47907 (e-mail: rickus@purdue.edu).

handling protocols. In addition, the solution phase nature of our method could be used in future work to mimic the chemistry found naturally in organisms such as diatoms to form hierarchical materials with ordered nano- and microstructure to more precisely control the mass transport, mechanical properties and stability of the encapsulant. The purpose of this paper is to evaluate the function of islets over time in culture after coating with a silica layer.

MATERIALS AND METHODS

Murine islet harvest and culture. Islets used for in vitro studies were harvested from 8- to 12-wk old CD-1 mice (Charles River, Wilmington, MA) using the procedure described in Stull et al. (43). Islet isolation studies were approved by the Indiana University Institutional Animal Care and Use Committees using AALAC guidelines. After harvest, islets were incubated at 37°C in RPMI 1640 medium supplemented with 10% fetal bovine serum, 100 U/ml penicillin, and 100 μg/ml streptomycin (Invitrogen, Carlsbad, CA) prior to encapsulation and analysis.

Human islet culture. Human islets were obtained from human cadaveric donors through the Integrated Islet Distribution Program (IIDP). All human material was deidentified and therefore IRB exempt based on criteria of and review by the Purdue Institutional Review Board. Human islets were handled using protocols approved by the Purdue Institutional Biosafety Committee. Upon arrival, islets were incubated at 37°C in DMEM (GIBCO 11054) supplemented with 10% fetal bovine serum, 100 U/ml penicillin, and 100 μg/ml streptomycin (Invitrogen) for 24 h prior to encapsulation and analysis.

Enriched silica solution preparation. Tetramethyl orthosilicate (TMOS, Sigma-Aldrich) was hydrolyzed in a 1:16 mol ratio (TMOS: H_2O) deionized water solution using 2.27 μl of 0.04 molar hydrochloric acid initiator per 1 g of solution. The mixture was stirred vigorously for 10 min until clear. The methanol produced by the hydrolysis reaction was removed from the solution by rotary evaporation under vacuum at 45°C (30% reduction in solution volume). The resulting saturated silica solution was refrigerated and used within 8 h of synthesis.

Islet encapsulation. Mouse islets suspended in culture medium were placed in a 15-ml centrifuge tube and pelletized using centrifugation. The medium was aspirated from the pellet. The islets were then resuspended in a silica mineralizing solution composed of 10 ml of α-MEM with L-glutamine medium (Mediatech, VWR), 500 μl of phosphate-buffered saline (Invitrogen), and 300 μl of enriched silica solution. Immediately after resuspension, the islets were transferred to a sterile 100-mm Petri dish and placed in an incubator for 15 min. After incubation, the mineralizing solution was gently aspirated from the islets and replaced with 10 ml of fresh warm (37°C) α-MEM to halt silica deposition. Encapsulated islets were returned to the incubator for 4 h to stabilize the mineral layer. The α-MEM medium was then removed and replaced with 10 ml of fresh RPMI culture medium. Samples of encapsulated islets were incubated for up to 28 days, with fresh medium exchange 2–3 times/wk, prior to analysis.

Human islets were encapsulated using a similar procedure. To determine the optimal encapsulation time, islets were exposed to mineralizing solution for 9, 12, or 15 min. After exposure, the mineralizing medium was removed and replaced with serum-free α-MEM for 4 h followed by medium exchange with DMEM-based human islet medium. A subpopulation of encapsulated islets was placed in murine RPMI culture medium to determine the effect of medium type on secondary biomineralization.

Scanning electron microscopy. Encapsulated mouse islets incubated for 0, 1, 2, 4, 7, and 14 days and human islets incubated for 0, 2, 7, and 14 days were immersed in a 4% glutaraldehyde-sterile phosphate buffer solution for 1 h at room temperature. The samples were then dehydrated using a series of ethanol solutions (25, 50, 75, 90, and 100%, respectively, 20-min exposure). Upon removal from the final ethanol wash, the samples were gently pipetted onto a scanning electron microscopy (SEM) sample post covered in carbon tape. Residual ethanol was removed, and the islets were allowed to dry for 12 h. Samples were then placed in a desiccating chamber prior to SEM imaging using an FEI NOVA nanoSEM high-resolution FESEM.

Energy-dispersive X-ray spectroscopy. Encapsulated islets were fixed in 4% glutaraldehyde-sterile phosphate buffer solution for 1 h, washed in deionized water to remove residual medium, dehydrated, and mounted as previously described. The samples were then placed in a desiccating chamber prior to analysis using an OXFORD INCA 250 energy-dispersive X-ray detector (EDS). Spectra were collected from both surface scans and from point sources on the islet surfaces. Surface element composition is reported as atomic percentage (at%).

Self-referencing biosensor quantification of oxygen flux. Time-resolved metabolic flux was measured in single islets by oscillating an oxygen biosensor perpendicular to the islet/coating surface. This technique, known as self-referencing, converts concentration sensors into dynamic biophysical flux sensors for quantifying real-time cellular transport (26, 31, 36, 39). Analyte flux is calculated using Fick's first law of diffusion (25) by continuously recording differential concentration (ΔC) while oscillating the microsensor between two locations separated by a fixed excursion distance (ΔX). An optical oxygen sensor was constructed by immobilizing an oxygen-quenched fluorescent dye (platinum tetrakis pentafluoropheynl porphyrin) on the tip of a tapered optical fiber (tip diameter 5 μm) (29). Background flux was recorded in bulk medium at least 5 mm away from cellular material for 5 min. Flux at the islet/coating surface was measured in murine islets before encapsulation and 4 h, 1 day, 2 days, 7 days, and 21 days after encapsulation ($n = 3$). After 20 min of recording, a 1 mM bolus of potassium cyanide (KCN) was added to the medium to disrupt oxidative phosphorylation and abrogate islet metabolism as recording continued for another 20 min.

Cell viability imaging and quantification. Silica-coated mouse islets were exposed to a combination of CellTracker Green CMFDA (live cell), propidium iodide (PI; permeable membrane), and Hoechst 33342 (nucleic acid) stains (Invitrogen). Cells were first incubated in culture medium containing 10 μM CellTracker Green CMFDA stain for 30 min. The medium was then replaced with warm (37°C) serum-free medium supplemented with 1 μl/ml PI (1 mg/ml) and 2 μl/ml Hoechst 33342 (10 mg/ml) solutions. The cells were allowed to incubate for an additional 10 min prior to analysis by confocal microscopy. A Nikon C1+ confocal microscope with three laser lines for Hoechst 33342 (Ex/Em 405/525), CellTracker Green (Ex/Em 488/525) and PI (Ex/Em 561/595) was used to run confocal scans on murine islets. Images were acquired using a ×10 objective lens at 5-μm intervals along the vertical axis. The EZ-CI software package was used for image capture and processing. A Radiance 2100 MP Rainbow (Zeiss, Oberkochen, Germany) confocal/multiphoton microscope equipped with green HeNe, 4-line argon, and Mai Tai lasers was used to image human islets. Quantitative live/dead assay of human islets was also performed using a Cell Counting Kit-8 (CCK-8; Dojindo Laboratories, Japan).

Insulin assay. Coated islets were tested for insulin secretion according to the method reported by Chen et al. and Crim et al. (7, 8). Islets (50 islets/sample) were incubated in modified Krebs-Ringer buffer (KRB, 2.5 mM glucose) at 37°C for 1 h. The samples were then washed with fresh KRB (2.5 mM glucose) and incubated for an additional 1 h. After incubation, the samples were washed and incubated in a final KRB solution containing 25 mM glucose. The supernatant was collected from each glucose exposure condition. Insulin concentration was then measured using a mouse insulin standard enzyme immunoassay (EIA) ELISA kit (Mercondia, Uppsala, Sweden).

RT-PCR. Paired sets of 50 encapsulated (2–3 donor mice per pool, 4–10 pools per time point) and nonencapsulated control (2–3 donor

mice per pool, 3–10 pools per time point) were harvested from each pool at 0, 4, 2, 7, 14, 21, and 28 days. Islet samples were washed with PBS and placed into 350 μl of RLT buffer with 1% β-mercaptoethanol. Both coated and uncoated islets were then mechanically lysed and the samples stored at −80°C prior to analysis. RNA was processed using an RNeasy kit (Qiagen, Valencia, CA). After purification, a 20-μl reaction volume of MMLV reverse transcriptase and random hexamers (Invitrogen) was used to convert 5 μl of total RNA into cDNA. Quantitative real-time PCR was then used to determine the expression of *Tbp*, *Actb*, *Ins-1/2*, *Pdx1*, *Nos2*, and *pre-Ins2*. Three microliters of the cDNA reaction (5-fold diluted) was used as a template for PCR. A 22-μl reaction volume containing Jump Start Taq-Polymerase (Sigma-Aldrich, St. Louis, MO) and gene-specific primers was added to the cDNA (25 μl total volume) according to the method of Chakrabarti et al. (6). SYBR Green probes purchased from Applied Biosystems (Carlsbad, CA) were used according to the manufacturer's instructions. All samples were run (Eppendorf Mastercycler Realplex Thermal Cycler, Hauppauge, NY) in at least triplicate (n = 3–10 replicates) and normalized to the expression levels of the *Tbp* housekeeping gene. Primers described previously include *Ins-1/2* (20), *pre-Ins2* (20), and Nos2 (44). For amplification of *Pdx1* the 5′-CGGACATCTCCCCATACGAAG-3′ (forward) and 5′-CCCCAGTCTCGGTTCCATTC-3′ (reverse) primers were used. Gene expression of *Actb, Ins-1/2*, *Pdx1*, *Nos2*, and *pre-Ins2* was evaluated by the $2^{-\Delta\Delta C_T}$ method and presented as fold up/down of transcripts of the respective genes relative to control (8).

Macrophage cytokine release assay. Encapsulated and nonencapsulated islets were cocultured with macrophages, and TNF-α release was measured. RAW 264.7 macrophages were obtained as a gift from Prof. Janice Blum at Indiana University of Medicine and seeded at a density of 50,000 cells/cm^2 onto a 24-well plate in DMEM supplemented with 10% fetal bovine serum and 1% penicillin-streptomycin. The cells were incubated in the plate for 24 h after seeding. After 24 h, the plate was rinsed with fresh medium to remove nonadherent macrophages. Fresh DMEM containing lipopolysaccharide (LPS, 100 ng/ml) was then added to each well, and the cells were allowed to activate for another 24 h. After 24 h, LPS was completely removed from the plate by rinsing the wells several times with PBS. Fifty encapsulated or nonencapsulated islets were added into each well with 1 ml of islet culture medium. After 1, 3, or 5 days of coculture incubation, the medium from each well was collected and replaced with a fresh medium. To determine TNF-α content secreted by the activated macrophages, the collected medium after each time point was measured by an enzyme-linked immunosorbent assay (ELISA) kit (R&D systems, Minneapolis, MN) following the manufacturer's instructions.

Transplantation of encapsulated islets into diabetic mice. Male C57BL/6J mice (8–12 wk old) were purchased from Jackson Lab (Bar Harbor, ME) and used as both recipient and donor mice. Recipient mice were rendered diabetic by one (180 mg/kg) or two (125 mg/kg) intraperitoneal injections of streptozocin (Sigma-Aldrich) 5 days prior to transplantation. Blood glucose was monitored daily after the injection, and mice were determined hyperglycemic when their minimal glucose level was >18 mmol/l for 2 consecutive days before transplantation. Prior to transplantation, anesthesia of recipient mice was induced and maintained by isoflurane. Five hundred encapsulated or nonencapsulated islets were pelletized by centrifugation and transplanted under the kidney capsule. After transplantation, glucose levels of each recipient mouse were measured every other day with an AlphaTrak blood glucose monitoring system (AlphaTrak; Abbott, Chicago, IL).

RESULTS

A thin silica coating forms at the surface of mouse and human islets. After exposure to the silica mineralizing medium for 15 min, a thin, smooth silica membrane coating was observed at the surface of mouse islets and human islets. EDS confirmed the presence of silica by the emergence of a silicon peak that was not present in control islets (Fig. 1).

To visualize the thickness of the layer, we intentionally disrupted the coating with a harsh series of alcohol dehydration and centrifugation, cracking the silica to partially expose the islet surface (Fig. 2). This method illustrated a silica layer thickness on the order of micrometers. A comparison of elemental content in this cracked sample confirmed a 4.03 at% Si over the shell and 0.72% residual Si at the underlying exposed islet surface (Fig. 2).

Similarly, human islets also formed a thin silica shell after exposure to saturated silica medium. SEM indicated that a silica layer was deposited on the surface of human islets after exposure to silica medium. EDS of samples exposed for 9 (n = 21), 12 (n = 17), or 15 (n = 10) min produced Si surface concentrations of 0.93 ± 0.07, 1.03 ± 0.12, and 0.75 ± 0.06 at% (±SE) respectively.

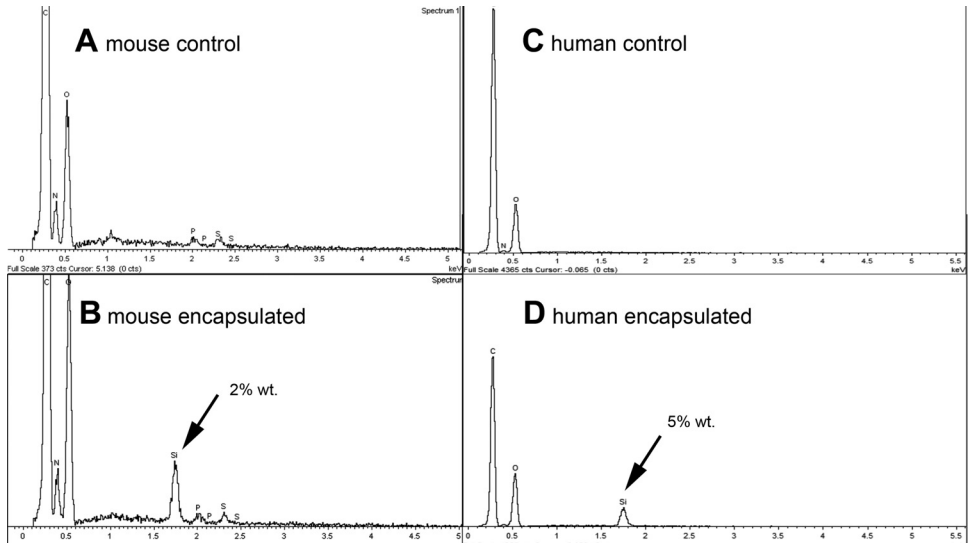

Fig. 1. Energy-dispersive X-ray (EDS) spectra of mouse and human islets show emergence of significant silicon peak at islet surface 4 h after exposure to silicification medium. Unexposed mouse (*A*) and human (*C*) control islets show no detectible level of silicon. Mouse (*B*) and human (*D*) islets showed a silicon peak after culture that in general ranged from 1 to 8% by weight relative to other detectible elements (typically C, O, N, S, P).

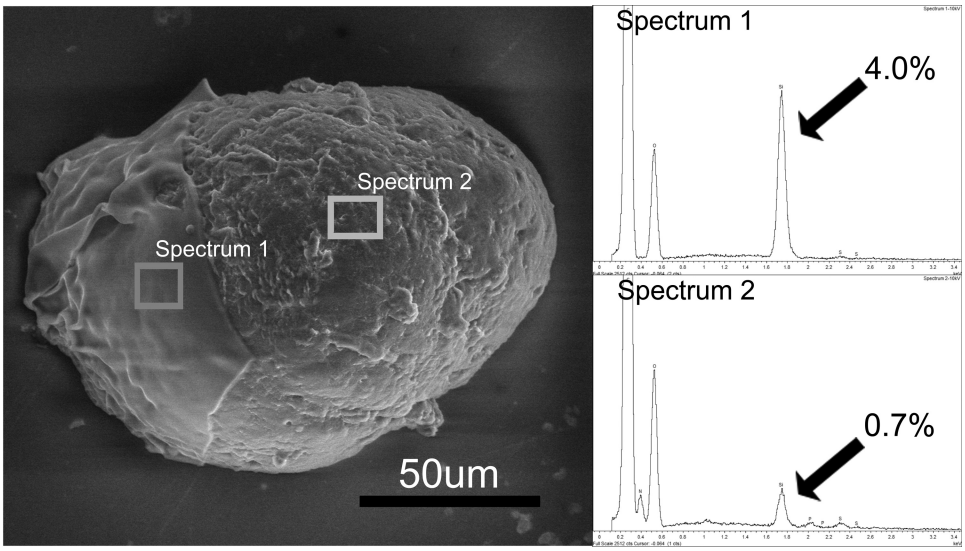

Fig. 2. Scanning electron micrograph (SEM) image of a mouse islet with a silica coating that was partially removed to reveal the underlying islet (right portion of islet). EDS *spectrum 1* was taken from a region where the coating remained in place (*left*) and had a silicon peak corresponding to 4.0 atomic% (8.6% by weight). EDS *spectrum 2* was taken from a region where the coating was removed (*right*) and had a silicon peak of 0.7 atomic% (1.5% by weight).

Silica-coated islets form secondary calcium phosphate layers over time when cultured in RPMI but not DMEM medium. To understand how the coating was affected by time in culture, we monitored the elemental composition of the islet coating on mouse islets, using SEM and EDS over a period of 14 days. Over time in RPMI medium, the coated islet surface formed a new layer comprised of calcium and phosphate (CaP) (Fig. 3). A calcium and phosphate peak emerged in the EDS spectra by 4 days in culture. The at%s of these elements were around 4 and 3%, respectively, and began to level off at around 8 and 5% after 2 wk in culture (Fig. 4). This result is consistent with a secondary biomineralization event in which silica present on the cell surface nucleated the deposition of a calcium phosphate (CaP) layer from the medium.

At 4 days (Fig. 3*A*), the coating displayed a rounded granular morphology indicative of amorphous CaP. Over time, the CaP layer continued to mature, transitioning to a form that visually appeared more crystalline (Fig. 3*B*). The ratio of calcium to phosphorus (Ca/P) can be used to infer the degree of crystallinity of the deposit (15, 22). Point source EDS analysis of the elemental composition of the CaP layer displayed a Ca/P ratio of 1.37 at the 4 day time point (Fig. 4, inset). Materials having a ratio $\leq$1.5 are usually considered to be amorphous. By day seven the Ca/P ratio increased to 1.42. By the 14-day time point, CaP apatite crystals (Ca/P = 1.67) completely covered the islet surface.

We hypothesized that the difference between mouse and human islets was due to the differences in their standard medium conditions. To test the effect of medium conditions, we cultured human islets in mouse medium (RPMI) after encapsulation and compared them to coated human islets cultured in DMEM. Incubation of silica-coated human islets in RPMI resulted in the formation of a secondary CaP layer in encapsulated human islets (Fig. 5), similar to that observed for mouse islets.

Biomineralized mouse and human islets cells survive encapsulation and culture. Fluorescence microscopy was used to observe mouse and human islet stress and survival after encapsulation (Fig. 6). At 4 h after encapsulation, PI-positive-stained cells were apparent relative to preencapsulation control islets; however, the majority of the islets were positive for live cells. By *day 2*, the number of PI-positive cells decreased comparable to the control sample, indicating that either dead cells or cellular debris had dissipated into the medium or that membrane damage was repaired. Importantly, we did not observe indications of a necrotic core.

Imaging of human islets revealed a small number of PI-permeable cells distributed evenly throughout the islet (Fig. 7).

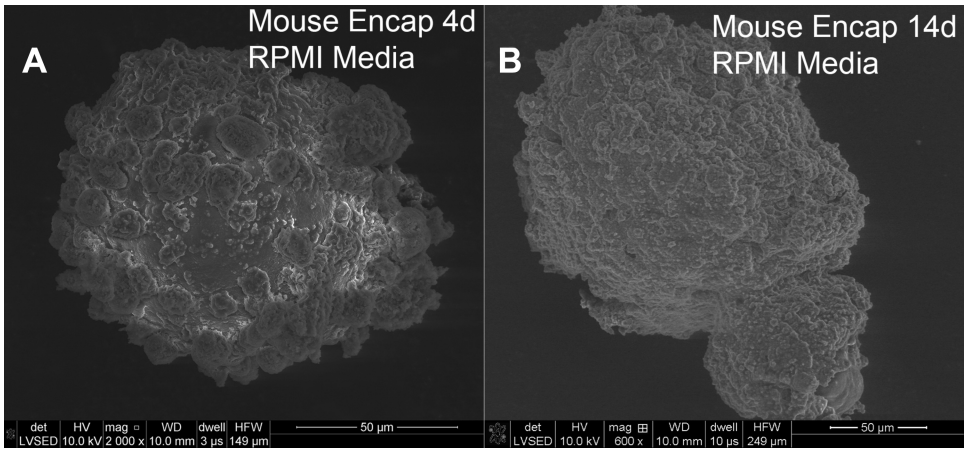

Fig. 3. After several days in culture in RPMI, mouse islets form a secondary calcium phosphate (CaP) layer. At 4 days posttreatment (*A*), granules of CaP could be seen on the surface of the islets. By 14 days (*B*), this layer completely covered the islets surface.

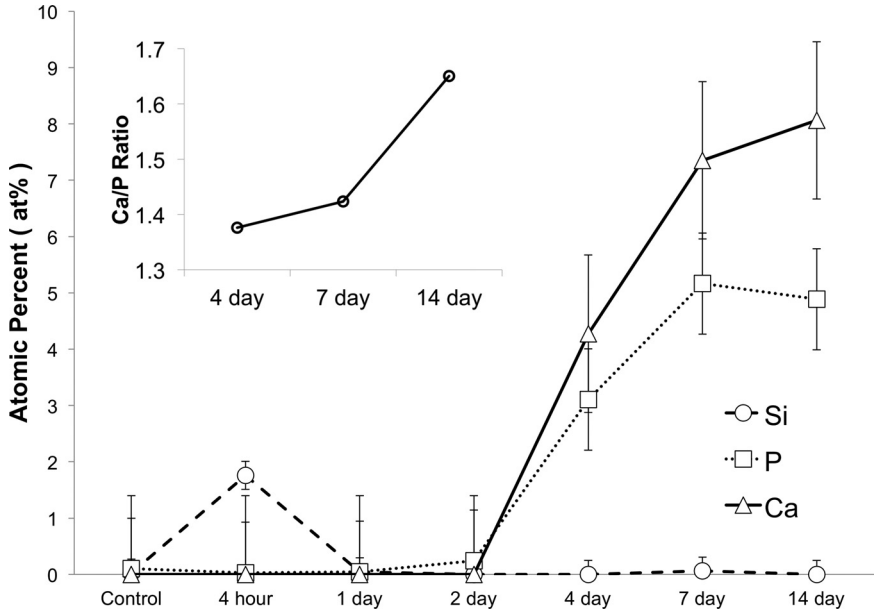

Fig. 4. CaP formation begins after 2 days in culture for silica-coated mouse islets. EDS analysis confirms initial formation of a silica deposit followed by growth of a CaP mineral layer upon incubation in RPMI. Concentration of the elements Si, Ca, and P at the encapsulated murine islet surface after 4 h ($n = 7$), 1 day ($n = 4$), 2 days ($n = 9$), 4 days ($n = 9$), 7 days ($n = 7$), and 14 days ($n = 4$) of incubation are shown vs. time in culture. Point source scans at CaP nodules at 4 days ($n = 9$), 7 days (=4), and 14 days ($n = 8$) show an increasing Ca/P ratio (*inset*) (atomic% ± SE).

Quantification of islet cell viability in human islets by a dehydrogenase activity-based assay kit showed a possible but not statistically significant decrease in cell viability immediately after encapsulation (Fig. 7*C*). Interestingly, by *day 2*, silica-coated human islets had a greater proportion of viable cells relative to control islets. This improved viability persisted at 7 days in culture.

Biomineralized mouse islets actively take up oxygen after encapsulation. We used a self-referencing oxygen optrode to measure oxygen flux at the surface of the mouse islet before and at varying times after silica encapsulation (Fig. 8). At each time point, we measured background flux (away from the cell), flux at the surface, and after treatment with KCN. The islets were treated with KCN to inhibit cellular respiration and confirm the cellular nature of the measured flux. KCN significantly reduced the flux at the islet surface in all cases. Control mouse islets on *day 0* had an average oxygen flux of 55.8 ± 12.3 pmol·cm^{-2}·s^{-1}. Immediately after encapsulation, the measured flux in mouse islets was reduced but remained unchanged in in culture over time.

Mouse islets retain glucose-stimulated insulin release after coating with silica. A comparison of glucose-stimulated insulin release showed few differences between control and encapsulated mouse islets over time (Fig. 9). Immediately after encapsulation, the encapsulated islets released more insulin at low glucose relative to controls (Fig. 9*A*); however, by 2 days, the basal release at low glucose was the same as control. At 28 days, silica-coated islets had significantly lower basal insulin release. When stimulated with high glucose, encapsulated and control islets showed similar release levels at all time points except at 7 days. No statistical difference in relative insulin release (ratio of release at high glucose to release at low glucose) was observed between control and encapsulated mouse islets at any time point after encapsulation (Fig. 9*C*). Both control and encapsulated islets demonstrated a relatively low stimulation index (≈2) at the *0-* and *2-day* time points (corresponding to 1 and 3 days postharvest). By 7 days after encapsulation (8 days postharvest), both encapsulated and control islets displayed a stronger stimulation index (≈8),

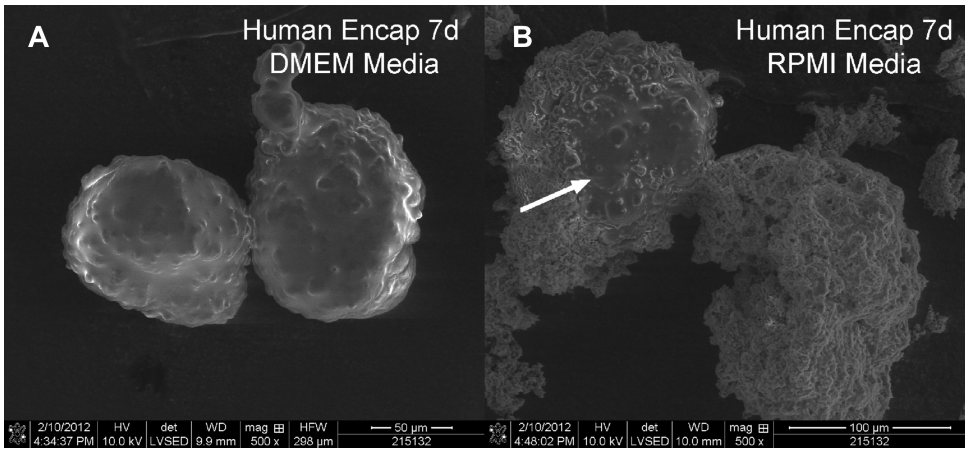

Fig. 5. Human islets do not form CaP layers when cultured in DMEM. SEM of human islets after silica coating followed by 7 days of culture in different media conditions. Human encapsulated islets incubated in DMEM (*A*) do not form a secondary CaP layer, whereas those incubated in RPMI (*B*) develop CaP deposits. White arrow indicates portion of exposed islet surrounded by the CaP encapsulant.

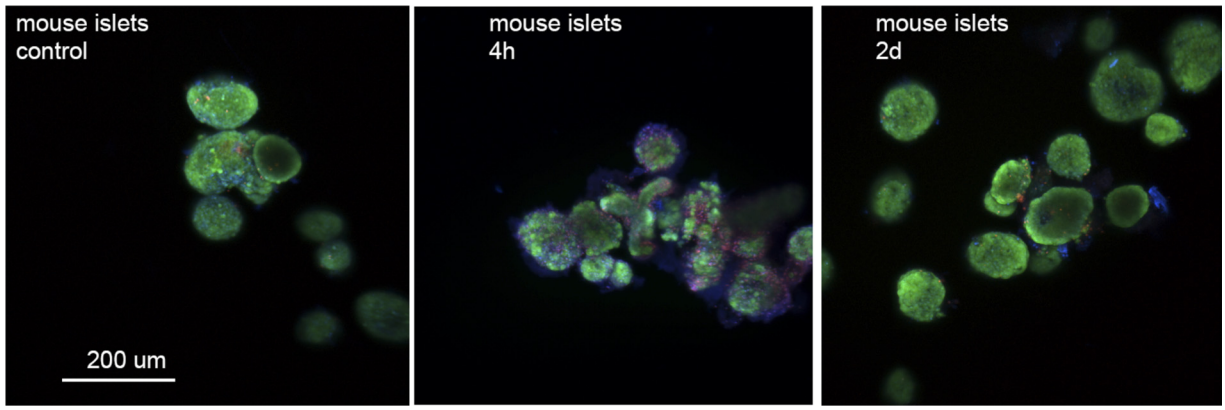

Fig. 6. Confocal imaging reveals some dead or membrane-permeable cells in mouse islets 4 h after coating that disappear by *day 2* in culture. Islets were stained with CellTracker Green CMFDA (live cell, green), propidium iodide (PI; permeable membrane, red), and Hoechst 33342 (nucleic acid, blue) stains. Images are overlaid Z stacks of 19–24 images. Scale bar, is 200 μm for all 3 images.

which was maintained for the duration of incubation up to 28 days.

Biomineral encapsulation does not significantly alter expression of β-cell-associated genes in mouse islets. We measured transcript levels of β-actin (*Actb*), and β-cell-associated transcripts, *Pdx1,* preinsulin (*pre-Ins2*), and insulin (*Ins-1/2*) by using the housekeeping gene *Tbp* as a reference (Fig. 10). Again, we found very few differences between control and silica-coated mouse islets at all times after encapsulation. Levels of *pre-Ins2* and *Pdx1* transcripts were reduced immediately after encapsulation but recovered by *day 2*. No differences in *Ins-1/2* transcript levels were observed at any time point.

Pdx1 is a β-cell-specific transcription factor associated with the regulation of several β-cell-specific genes (6). *Ins-1/2*, the transcript responsible for insulin production, is commonly associated with functional islets (2). *Ins-1/2* is expressed at high levels in insulin-producing cells and possesses a long half-life (17). The *pre-Ins*2 transcript exists at lower levels and has a faster turnover rate (17). Expression of pre-mRNA is therefore a good reference for acute changes in gene transcription, indicating that the cells are responsive to their environment (17). Taken together, these results indicate that alterations in functional gene expression of islets due to encapsulation are limited and temporary.

In addition to the β-cell-associated markers, inducible nitric oxide synthase (*Nos2*) transcript was measured as an indicator of cell stress in mouse islets (Fig. 11). Expression of *Nos2* increased immediately after biosilicification in some but not all samples, resulting in a high variability at the 0 time point. By 4 days, *Nos2* transcripts returned to levels that were indistinguishable from control levels for the remainder of the culture period. The apparent differences in averages at 0 and 2 days failed tests for significance and were driven primarily by one or two samples with high *Nos2* measurements. This result may reflect variability in the handling of the islets during the biomineralization process.

Silica-coated islets increase TNF-α levels in macrophage coculture. To investigate the response of macrophages to silica-coated islets, we cocultured encapsulated and nonencapsulated islets with macrophages and measured TNF-α protein levels at *days 1, 3,* and *5* (Fig. 12). The amount of TNF-α was not significantly different between the groups of macrophages cultured with nonencapsulated mouse islets and macrophages

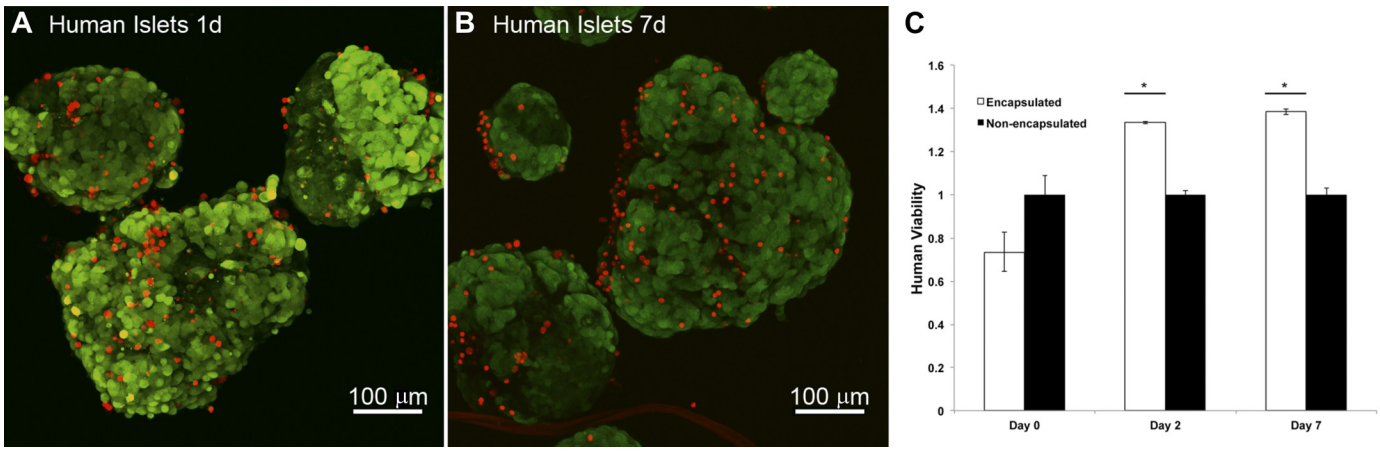

Fig. 7. Human islets are viable after silica coating and show improved viability in culture over time. Islets were stained with CellTracker Green CMFDA (live cell, green) and PI (red). Confocal imaging reveals even distribution of a few PI-permeable cells 1 day (*A*) and 7 days (*B*) after coating. *C*: islet viability of encapsulated human islets is reduced on the day of encapsulation but improved 2 and 7 days after encapsulation. *$P < 0.01$ vs. groups of nonencapsulated islets. All data normalized to nonencapsulated human islet viability. Error bars, ±1 SE (n = 3–4 replicates per condition).

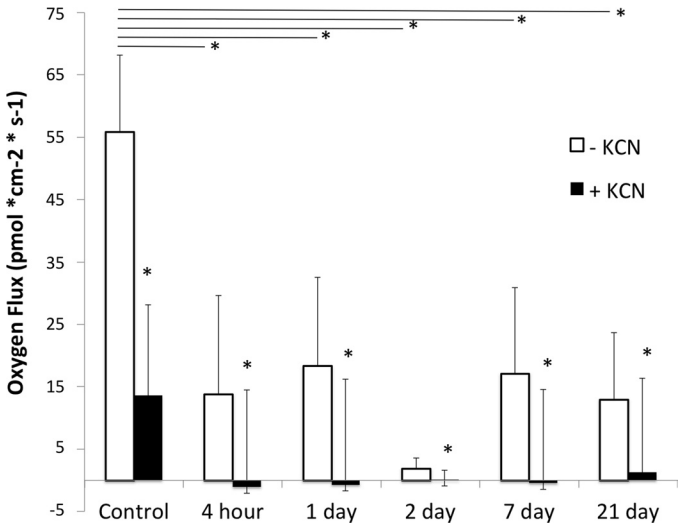

Fig. 8. Oxygen flux at the surface of mouse islets decreased after coating with silica but was stable over time in culture. Flux was measured perpendicular to the islet surface in nonencapsulated mouse islets on *day 0* (control, $n = 3$), 4 h ($n = 3$) after encapsulation, and 1 day ($n = 3$), 2 days ($n = 3$), 7 days ($n = 3$), and 21 days ($n = 4$) after encapsulation and culture. KCN was added during recording to inhibit cellular respiration and confirm cellular source of the measured flux. Open bars, before KCN treatment; filled bars, after KCN treatment; error bars, SD. *Significant difference at $P < 0.05$.

cultured alone. However, when cocultured with biosilica-encapsulated islets, macrophages released more TNF-α than when they were cocultured with nonencapsulated islets and when they were cultured alone. This result was consistent for all time points examined. As a positive control, macrophages were stimulated with LPS under all conditions (alone, cocultured with nonencapsulated mouse islets, and cocultured with encapsulated islets). A similar trend was observed when macrophages were already stimulated with LPS. That is, the amount of TNF-α secreted from macrophages with encapsulated islets was highest among the three groups.

Encapsulated biosilica islets reverse hyperglycemia in diabetic mice after syngeneic transplantation. To investigate whether the silica-encapsulated islets could survive and function in vivo, syngeneic transplantation was performed in C57BL/6J mice made diabetic by STZ injection. Figure 13 shows blood glucose levels of the recipient diabetic mice implanted with 500 encapsulated or control islets after transplantation. Encapsulated islets could reinstate normal glucose control in mice as well as or better than nonencapsulated islets.

DISCUSSION

Silica is a proven material for protein separation and exclusion. Material scientists have developed methods to create hierarchical silica structures with well-defined nano- and microscale pores to precisely control mass transport and mechanical properties. By far the majority of these methods use conditions such as high temperature treatment or solvent exchange that are completely incompatible with living cells. Our long-term goal is to translate and adapt the materials chemistry of mesoporous silica to the cell and islet surface so that we can create precision separation materials as an islet encapsulant. Biological organisms such as diatoms and sponges create such silica materials under physiological conditions and serve as inspiration.

This work is a first step in achieving our goal and the first demonstration of using the islet surface itself as a template for silica synthesis in aqueous conditions. We showed that we could grow thin films on both mouse and human islets. Previously, we demonstrated similar results by exposing *Pseudomonas aeruginosa* and *Nitrosomonas europaea* biofilms to a saturated silica solution, forming a silica layer that reduced cell detachment from bacterial biofilms under fluid flow (21). The formation of a similar bioencapsulant by four different multicellular structures suggests a common mechanism that may be adaptable to many different tissue types. Extracellular membranes and matrices are studded with proteins and polysaccharides containing hydroxyl (-OH) groups. We hypothesize that such hydroxyls, which can participate in hydrogen (4, 18) and covalent (23, 24) bonding with silicic acid molecules, serve as a site for silica polycondensation at the tissue surface.

Our goal in this paper was to evaluate islet survival and function in culture after silica coating. Cell staining, oxygen flux measurements, stimulated insulin release, gene expression, viability assays, and in vivo transplants all showed that the

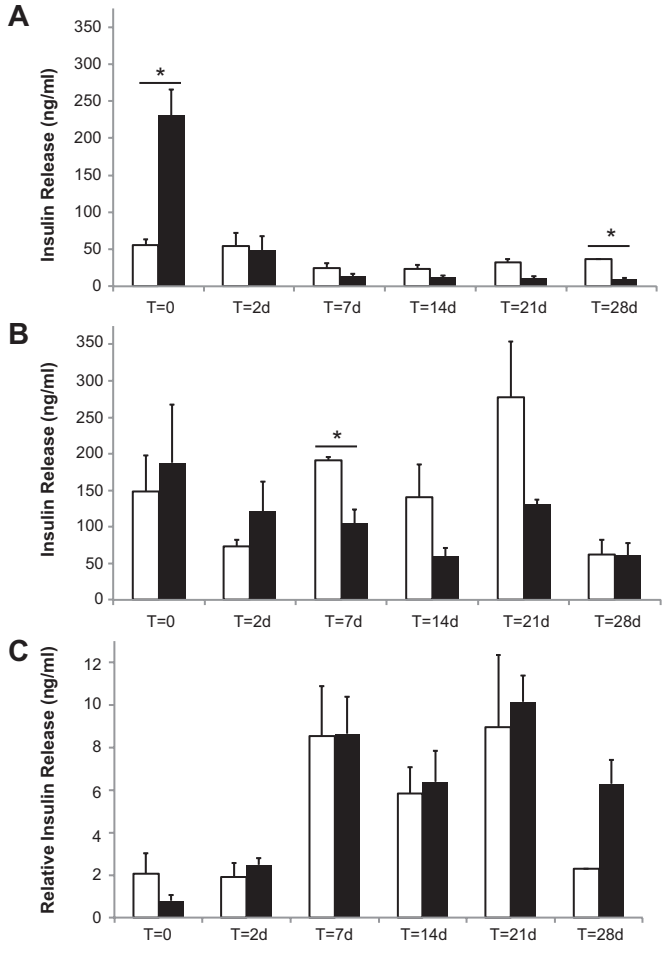

Fig. 9. Glucose-stimulated insulin release from biomineralized (silica-coated) mouse islets. Insulin release from encapsulated mouse islets (filled bars) is comparable to that of control mouse islets (open bars) when stimulated with low (*A*) and high (*B*) glucose at varying times after encapsulation. $T = 0$ corresponds to immediately after encapsulation. *C*: relative insulin release is the ratio of insulin released at high glucose relative to low glucose. Data are presented as average ± SD. *Significant differences between pairs, $P < 0.05$.

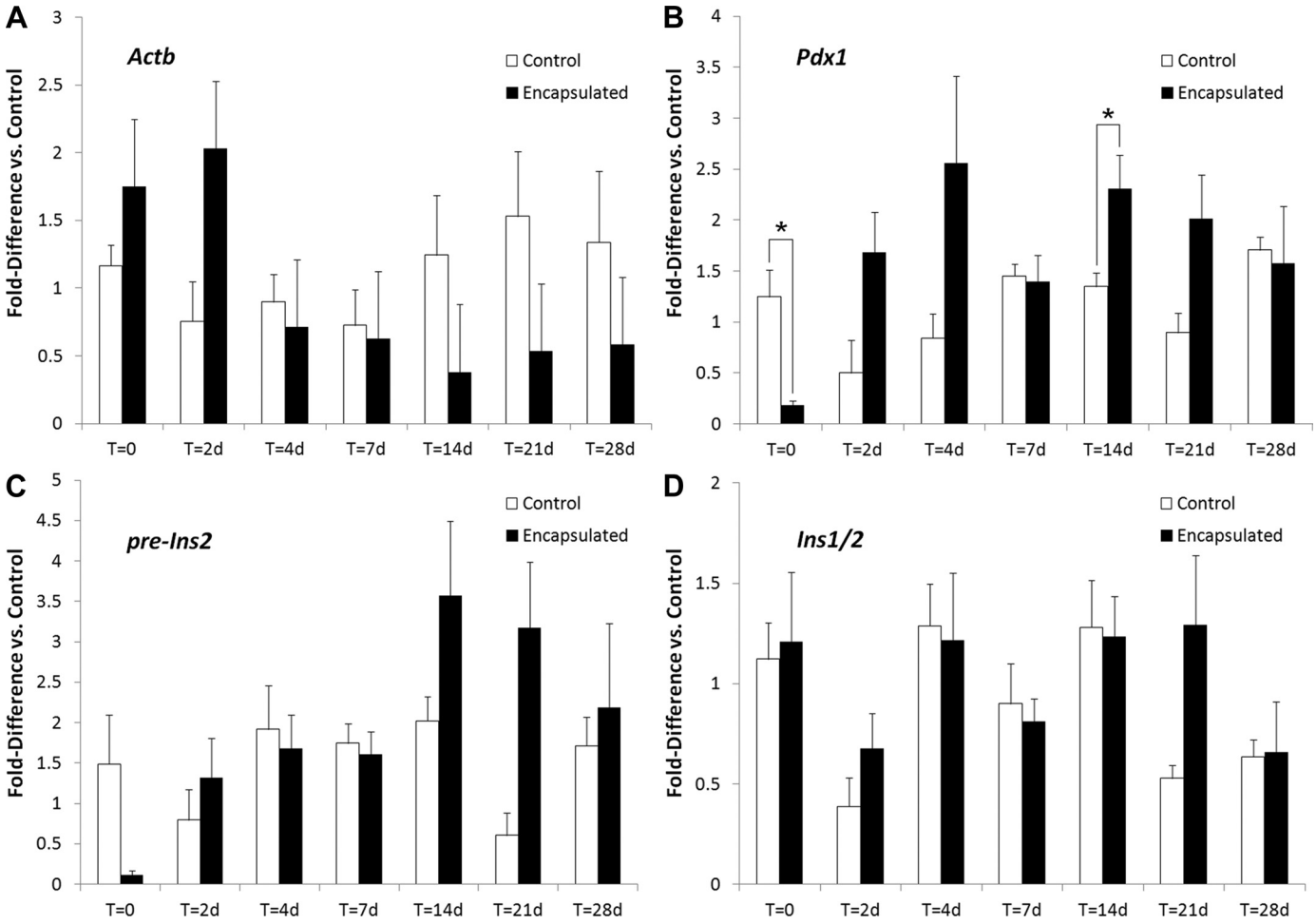

Fig. 10. Silica coating of mouse islets does not alter transcript levels of β-cell-associated genes. Real-time PCR analysis indicates that encapsulated islets retain gene expression levels, consistent with those of nonencapsulated controls. Quantification of gene regulation for (*A*) Actb (cytoskeletal element), (*B*) Pdx1 (β-cell-specific gene regulator), (*C*) pre-Ins2 (insulin gene pre-mRNA), and (*D*) Ins1/2 (gene encoding insulin) was conducted. All data are presented as fold up/downregulation of transcripts of respective genes relative to the Tbp housekeeping gene. *Significant ($P \leq 0.05$) relative to nonencapsulated controls at the respective time point. All sample pairs were analyzed by one-way ANOVA. Error bars, ±1 SE (n = 3–10 replicates per condition).

silica coating is compatible with islet survival and function in culture for several weeks.

Although we largely saw good survival and function, there were indications in the 4-h data, such as PI-positive cells and decreased *Pdx1* expression, that the islets may experience some stress during the coating process. In contrast, insulin transcripts were not affected by encapsulation, and glucose-stimulated insulin release was indistinguishable from controls. This stress could be caused by physical manipulation, exposure to the silica-forming medium, or the formation of the material itself. Any stress on the cells during the 5- to 15-min exposure to the silica medium sol could be due to the silica monomer, reduced pH that occurs during polycondensation, residual methanol if methanol was not completely removed prior to forming the sol, or physical agitation during handing of the cells.

Interestingly, expression of inducible nitric oxide synthase, *Nos2,* a sensitive responder to islet stress (28), was not significantly different between encapsulated islets and controls, although a few of the many encapsulated islet samples did have high *Nos2* levels. This finding could be due to variability in the encapsulation process indicating that automation or optimization of the silicification might reduce these effects.

In contrast, at later time points, encapsulated islets performed as well as or better than control islets in culture. Basal insulin release at low glucose levels was lower for encapsulated mouse islets than for controls at 28 days, and *Pdx1* expression was higher for encapsulated mouse islets at 14 days. In addition, the data presented may actually underestimate this result. Although not quantified, a high attrition rate was observed in nonencapsulated control mouse islets over time. After 14 days of incubation, we observed that ~50% of the initial pool of islets died in vitro, a phenomenon commonly observed in long-term culture. Only surviving islets were available for sample collection, potentially biasing the control data set. Encapsulated islets did not experience as high rates of attrition. We observed apparent islet numbers remained at ~80–90% of initial concentrations over the course of 3–4 wk. This observation was quantified for human islets where we measured an ~40% increase in numbers of viable cells for coated islets at 2 and 7 days in culture. We hypothesize that providing the islets with a biomineral coating creates a 3D

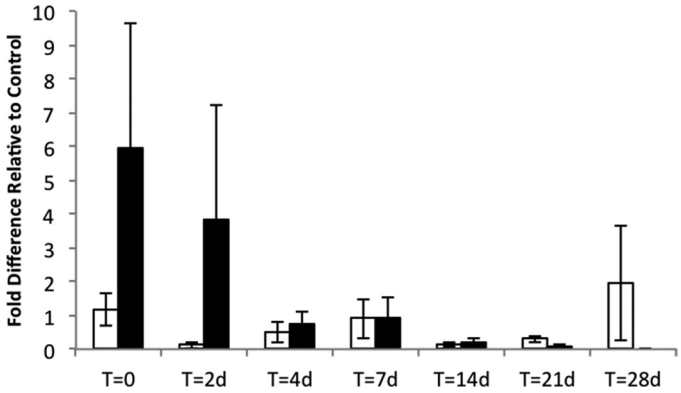

Fig. 11. Silica coating does not alter expression of *Nos2* transcript levels. *Nos2* transcript expression in encapsulated mouse islets (filled bars) vs. nonencapsulated islets (open bars) measured at varying time points after encapsulation. $T = 0$ corresponds to immediately after encapsulation. Data are presented as fold increase relative to the Tbp housekeeping gene. All sample pairs were analyzed by one-way ANOVA. Error bars, ±1 SE (n = 3–10 replicates per condition).

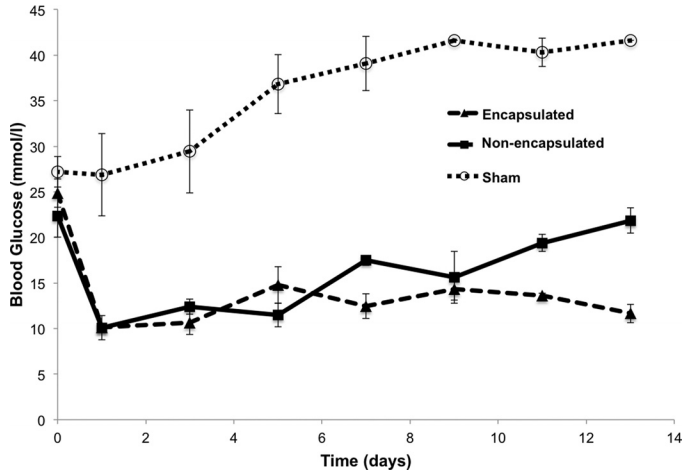

Fig. 13. Silica-coated islets reverse hyperglycemia after syngeneic transplant in diabetic mice. Blood glucose of STZ-induced diabetic mice after beingtransplanted with 500 encapsulated islets (encapsulated), nonencapsulated islets (nonencapsulated), or saline (Sham). Error bars, ±1 SE (n = 3, 2, and 4 replicates in groups of encapsulated, nonencapsulated, and sham, respectively).

support matrix for the islets in culture, improving their long-term survival. Future work will investigate this hypothesis more directly.

Taking all of the results into account, we conclude that the stress experienced by the islets is limited and temporary; however, future work may be directed at completely eliminating this stress as we optimize the coating procedures.

Interestingly, we saw that the silica was bioactive under certain media conditions. While biosilica mouse islets readily experienced secondary biomineralization by CaP formation, human islets did not form CaP when cultured in standard human islet medium. Several factors could influence the medium's ability to form precipitates, including serum protein levels, glucose concentration, pH, temperature, and the concentration of calcium and phosphate ions. DMEM contains 1.8 mM Ca^{2+} and 0.906 mM PO_4^{-}, whereas RPMI contains 0.848 mM Ca^{2+} and 5.64 mM PO_4^{-}. This difference in ion balance, alone or coupled with other factors such as higher glucose concentration, may have allowed RPMI medium to form silica-induced CaP mineral deposits.

There are several potential consequences of calcification in mouse media. First and foremost, we must determine whether this secondary biomineralization occurs in vivo. Because the CaP formation was highly dependent on the media conditions, the in vivo bioactivity may also depend on transplant site. In addition, we may need to alter the media conditions for mouse islets to prevent CaP formation in culture prior to transplantation or transplant soon after coating with silica. Such alterations may not be required for silica-coated human islets; however, this result will need to be confirmed with human

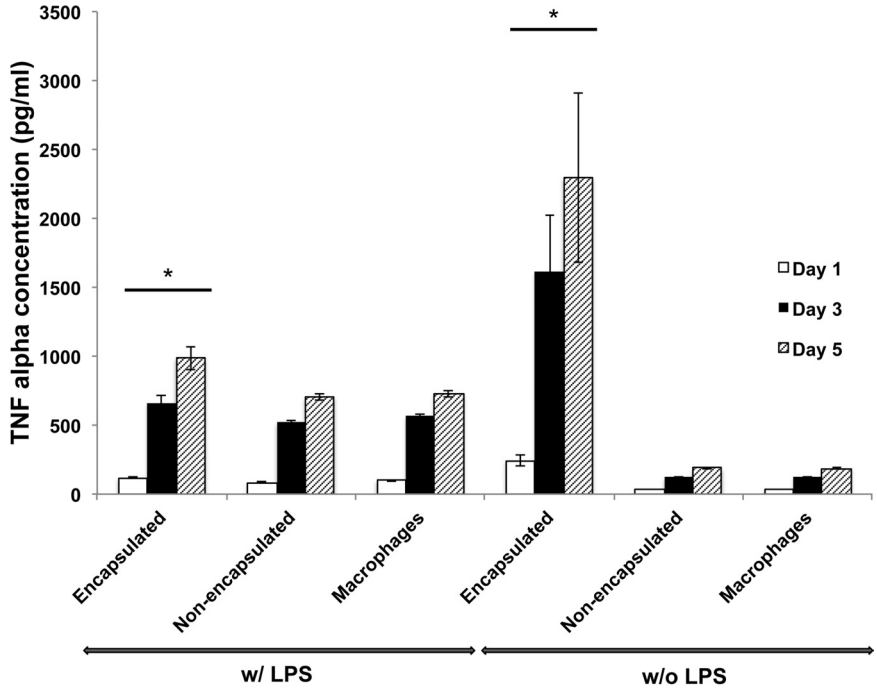

Fig. 12. Encapsulated islets stimulate TNF-α release by macrophages. Extracellular TNF-α protein was measured when macrophages were cocultured with biosilica islets (encapsulated), control islets (nonencapsulated), and when cultured alone (macrophages) with or without activation of LPS. *$P < 0.01$ vs. groups of nonencapsulated islet-macrophages and macrophages only. Error bars, ±1 SE (n = 3 replicates per condition).

media supplements as opposed to the FCS, which was used here.

From a different point of view, the bioactivity of silica may be an advantage for transplanted islets. Unlike traditional encapsulant materials, which are generally designed to interact as little as possible with the body, bioactive glasses integrate with surrounding tissues and could reduce the formation of granulation tissue and a fibrous capsule around the transplant. This type of bioactivity has been used in hard-tissue reconstruction. Silica-based bioactive glasses, such as type 45S5 (46.1 SiO_2 - 24.4 Na_2O - 26.9 CaO - 2.6 P_2O_5, mol%), are used to fill bone defects and improve bone-tissue interfaces (46, 47). Studies have demonstrated that conditioned medium, composed of 45S5 dissolution products and CCD-18Co human fibroblast cellular products generated from exposure to particulate 45S5, significantly increases human dermal microvascular endothelial cell proliferation relative to tissue culture-plastic controls (10). In future work, we may be able to exploit these properties in vivo to generate an islet encapsulant that rapidly binds to surrounding tissues, improving diffusion to the implant by integrating with the surrounding microvasculature system. Because one of the primary failure modes of encapsulated islets is insufficient nutrient transport (11), biomineralization as a route to healthy tissue integration could potentially extend transplant lifetime while still providing a porous protective layer. Combining our approach with transplant into capillary-rich tissue may further improve survival by increasing oxygen availability and reducing hypoxia.

Our in vitro assay of biocompatibility indicated that the silica-coated islets can aggravate macrophages in culture to cause increased TNF-α levels. These levels were as high as or higher than LPS-induced activation. Surprisingly, encapsulated islets without LPS seemed to result in higher TNF-α levels than encapsulated islets plus LPS, a result for which we do not yet have full understanding. Future work may also need to examine TNF-α secretion from the islets themselves. Regardless, in vitro assays of the biocompatibility of biomaterials are not always good predictors of in vivo biocompatibility. In this case, we saw sufficient survival of transplanted islets in the time course of weeks, suggesting that in vivo inflammatory response was not a significant issue.

In our existing data set, oxygen transport into the cells from the medium appears to be reduced yet stable after encapsulation. This result could be due to reduced diffusivity of oxygen through the layer; however, the alternative conclusion is that the magnitude of the flux is simply decreased by the experimental artifact of an increased distance between the optrode and the islet. Flux is calculated from the concentration gradient, which theoretically and experimentally decreases with distance from the source or sink (30, 32), in this case the islet surface. The coating imposes at least one to a few micrometers distance between the islet and the surface of the coating and therefore the islet surface and the optrode. In future work, we will examine the transport properties of the material more directly as we optimize the pore structure for protection from the immune system. Regardless, we do not see evidence of a necrotic core in our observations by confocal microscopy, and the islets survive for weeks in vivo as indicated by restoration of normal blood glucose levels in diabetic mice.

While the work here demonstrates the compatibility of mouse and human islets with a biomineral shell, future work must test the protective capabilities of that shell. Layer porosity and diffusional properties of silica-based sol-gels can be altered by manipulation of a number of factors during the encapsulation process. Ongoing research is underway to improve the chemical and physical durability of the sol-gel layer, to optimize of the encapsulant system to maintain normal levels of nutrient diffusion and insulin transport while providing cytokine barrier function, and to continue to measure the in vivo behavior of silica-encapsulated islets. Proper design of a silica encapsulant could allow for good transport of insulin while protecting from even the smaller molecules of the immune attack such as cytokines. Importantly, many years of microencapsulation of islets with hydrogels, e.g., alginate, and more recently organic coatings such as PEG, have shown varying degrees of success and advantage (12–14, 19, 27, 41, 42, 45). One possible strategy is to incorporate the best material properties from the organic systems with the inorganic such as silica to create multifunctional hybrid composites. Given the complex and difficult nature of immunoprotection, such a multipronged strategy may have strength.

ACKNOWLEDGMENTS

We thank Dr. Deborah Sherman at the Purdue Life Sciences Microscopy Facility for assistance with SEM and EDS. We thank Drs. Sarah Tersey and Yurika Nishiki for assistance with quantitative PCR and Prof. Janice Blum for providing macrophage cells and guidance in their use. We acknowledge the Integrated Islet Distribution Program (IIDP) and the IIDP coordinating center at the City of Hope for access to human islets and the Indiana Diabetes Research Center Islet Core for access to isolated mouse islets.

GRANTS

This research was supported by the Indiana Clinical and Translational Sciences Institute, funded in part by Grant RR-025761 from the National Institutes of Health, National Center for Research Resources, Clinical and Translational Sciences Award; Wallace H. Coulter, Coulter Translational Research Award; and the Purdue Research Foundation Trask Fund. This work was also supported in part by National Institute of Diabetes and Digestive and Kidney Diseases Grants R01 DK-083583 (to R. G. Mirmira) and U01 DK-089561 (to M. C. Yoder).

DISCLOSURES

No conflicts of interest, financial or otherwise, are declared by the author(s).

AUTHOR CONTRIBUTIONS

Author contributions: D.B.J., J.L., R.M., R.G.M., and J.L.R. conception and design of research; D.B.J., J.L., R.M., N.D.S., M.S., J. Shi, J.L.K., R.H.-P., M.Z., and J. Sturgis performed experiments; D.B.J., J.L., R.M., N.D.S., M.S., J. Shi, J.L.K., R.H.-P., M.Z., J. Sturgis, and J.L.R. analyzed data; D.B.J., J.L., R.M., J.L.K., R.H.-P., J.P.R., M.C.Y., D.M.P., R.G.M., and J.L.R. interpreted results of experiments; D.B.J., J.L., R.M., and J.L.R. prepared figures; D.B.J., J.L., and J.L.R. drafted manuscript; D.B.J., J.L., R.M., J.L.K., J.P.R., M.C.Y., R.G.M., and J.L.R. edited and revised manuscript; D.B.J., J.L., R.M., N.D.S., M.S., J. Shi, J.L.K., R.H.-P., M.Z., J. Sturgis, J.P.R., M.C.Y., D.M.P., R.G.M., and J.L.R. approved final version of manuscript.

REFERENCES

1. **Barshes NR, Wyllie S, Goss JA.** Inflammation-mediated dysfunction and apoptosis in pancreatic islet transplantation: implications for intrahepatic grafts. *J Leukocyte Biol* 77: 587–597, 2005.
2. **Bengtsson M, Stahlberg A, Rorsman P, Kubista M.** Gene expression profiling in single cells from the pancreatic islets of Langerhans reveals lognormal distribution of mRNA levels. *Genome Res* 15: 1388–1392, 2005.
3. **Berney T, Toso C.** Monitoring of the islet graft. *Diabetes Metab* 32: 503–512, 2006.
4. **Birchall JD.** The role of silicon in biology. *Chem Brit* 26: 141–144, 1990.

5. **Carturan G, Dal Toso R, Boninsegna S, Dal Monte R.** Encapsulation of functional cells by sol-gel silica: actual progress and perspectives for cell therapy. *J Mater Chem* 14: 2087–2098, 2004.
6. **Chakrabarti SK, James JC, Mirmira RG.** Quantitative assessment of gene targeting in vitro and in vivo by the pancreatic transcription factor, Pdx1. Importance of chromatin structure in directing promoter binding. *J Biol Chem* 277: 13286–13293, 2002.
7. **Chen M, Yang ZD, Wu RP, Nadler JL.** Lisofylline, a novel antiinflammatory agent, protects pancreatic beta-cells from proinflammatory cytokine damage by promoting mitochondrial metabolism. *Endocrinology* 143: 2341–2348, 2002.
8. **Crim WS, Wu RP, Carter JD, Cole BK, Trace AP, Mirmira RG, Kunsch C, Nadler JL, Nunemaker CS.** AGI-1067, a novel antioxidant and anti-inflammatory agent, enhances insulin release and protects mouse islets. *Mol Cell Endocrinol* 323: 246–255, 2010.
9. **Davalli AM, Scaglia L, Zangen DH, Hollister J, BonnerWeir S, Weir GC.** Vulnerability of islets in the immediate posttransplantation period—dynamic changes in structure and function. *Diabetes* 45: 1161–1167, 1996.
10. **Day RM.** Bioactive glass stimulates the secretion of angiogenic growth factors and angiogenesis in vitro. *Tissue Eng* 11: 768–777, 2005.
11. **de Groot M, Schuurs TA, van Schilfgaarde R.** Causes of limited survival of microencapsulated pancreatic islet grafts. *J Surg Res* 121: 141–150, 2004.
12. **De Vos P, De Haan B, Wolters GH, Van Schilfgaarde R.** Factors influencing the adequacy of microencapsulation of rat pancreatic islets. *Transplantation* 62: 888–893, 1996.
13. **de Vos P, Hamel AF, Tatarkiewicz K.** Considerations for successful transplantation of encapsulated pancreatic islets. *Diabetologia* 45: 159–173, 2002.
14. **DeVos P, DeHaan B, Pater J, VanSchilfgaarde R.** Association between capsule diameter, adequacy of encapsulation, and survival of microencapsulated rat islet allografts. *Transplantation* 62: 893–899, 1996.
15. **Eanes ED, Gillesse IH, Gosner AS.** Intermediate states in precipitation of hydroxyapatite. *Nature* 208: 365–367, 1965.
16. **Emamaullee JA, Rajotte RV, Liston P, Korneluk RG, Lakey JRT, Shapiro AMJ, Elliott JF.** XIAP overexpression in human islets prevents early posttransplant apoptosis and reduces the islet mass needed to treat diabetes. *Diabetes* 54: 2541–2548, 2005.
17. **Evans-Molina C, Garmey JC, Ketchum R, Brayman KL, Deng SP, Mirmira RG.** Glucose regulation of insulin gene transcription and pre-mRNA processing in human islets. *Diabetes* 56: 827–835, 2007.
18. **Hecky RE, Mopper K, Kilham P, Degens ET.** Amino-acid and sugar composition of diatom cell-walls. *Marine Biol* 19: 323–331, 1973.
19. **Hobbs HA, Kendall WF, Darrabie M, Opara EC.** Prevention of morphological changes in alginate microcapsules for islet xenotransplantation. *J Invest Med* 49: 572–575, 2001.
20. **Iype T, Francis J, Garmey JC, Schisler JC, Nesher R, Weir GC, Becker TC, Newgard CB, Griffen SC, Mirmira RG.** Mechanism of insulin gene regulation by the pancreatic transcription factor Pdx-1. *J Biol Chem* 280: 16798–16807, 2005.
21. **Jaroch D, McLamore E, Zhang W, Shi J, Garland J, Banks MK, Porterfield DM, Rickus JL.** Cell-mediated deposition of porous silica on bacterial biofilms. *Biotechnol Bioeng* 108: 2249–2260, 2011.
22. **Kim S, Ryu HS, Shin H, Jung HS, Hong KS.** In situ observation of hydroxyapatite nanocrystal formation from amorphous calcium phosphate in calcium-rich solutions. *Mat Chem Phys* 91: 500–506, 2005.
23. **Kinrade SD, Gillson AME, Knight CTG.** Silicon-29 NMR evidence of a transient hexavalent silicon complex in the diatom Navicula pelliculosa. *J Chem Soc Dalton Trans* 307–309, 2002.
24. **Kinrade SD, Hamilton RJ, Schach AS, Knight CTG.** Aqueous hypervalent silicon complexes with aliphatic sugar acids. *J Chem Soc Dalton Trans* 961–963, 2001.
25. **Kuhtreiber WM, Jaffe LF.** Detection of extracellular calcium gradients with a calcium-specific vibrating electrode. *J Cell Biol* 110: 1565–1573, 1990.
26. **Land SC, Porterfield DM, Sanger RH, Smith PJS.** The self-referencing oxygen-selective microelectrode: Detection of transmembrane oxygen flux from single cells. *J Exp Biol* 202: 211–218, 1999.
27. **Lim F, Sun A.** Microencapsulated islets as bioartificial endocrine pancreas. *Science* 210: 908–910, 1980.
28. **Maier B, Ogihara T, Trace AP, Tersey SA, Robbins RD, Chakrabarti SK, Nunemaker CS, Stull ND, Taylor CA, Thompson JE, Dondero RS, Lewis EC, Dinarello CA, Nadler JL, Mirmira RG.** The unique hypusine modification of eIF5A promotes islet beta cell inflammation and dysfunction in mice. *J Clin Invest* 120: 2156–2170, 2010.
29. **McLamore ES, Jaroch D, Chatni MR, Porterfield DM.** Self-referencing optrodes for measuring spatially resolved, real-time metabolic oxygen flux in plant systems. *Planta* 232: 1087–1099, 2010.
30. **McLamore ES, Mohanty S, Shi J, Claussen JC, Jedlicka SS, Rickus JL, Porterfield DM.** A self-referencing glutamate biosensor for measuring real time neuronal glutamate flux. *J Neurosci Methods* 189: 14–22, 2010.
31. **McLamore ES, Porterfield DM, Banks MK.** Non-invasive self-referencing electrochemical sensors for quantifying real-time biofilm analyte flux. *Biotechnol Bioeng* 102: 791–799, 2009.
32. **McLamore ES, Shi J, Jaroch DB, Barcus C, Osbourne J, Uchida A, Jiang Y, Buhman KK, Banks K, Teegarden D, Rickus JL, Porterfield DM.** A self referencing enzyme-based microbiosensor for real time measurement of physiological glucose transport. *Biosens Bioelectron* 2010.
33. **Muraca M, Vilei MT, Zanusso E, Ferraresso C, Granato A, Doninsegna S, Dal Monte R, Carraro P, Carturan G.** Encapsulation of hepatocytes by SiO2. *Transplant Proc* 32: 2713–2714, 2000.
34. **Peterson KP, Peterson CM, Pope EJA.** Silica sol-gel encapsulation of pancreatic islets. *Proc Soc Exp Biol Med* 218: 365–369, 1998.
35. **Pope EJA, Braun K, Peterson CM.** Bioartificial organs 1. Silica gel encapsulated pancreatic islets for the treatment of diabetes mellitus. *J Sol-Gel Sci Technol* 8: 635–639, 1997.
36. **Porterfield DM.** Measuring metabolism and biophysical flux in the tissue, cellular and sub-cellular domains: recent developments in self-referencing amperometry for physiological sensing. *Biosens Bioelectron* 22: 1186–1196, 2007.
37. **Rabinovitch A, Suarez-Pinzon WL.** Cytokines and their roles in pancreatic islet beta-cell destruction and insulin-dependent diabetes mellitus. *Biochem Pharmacol* 55: 1139–1149, 1998.
38. **Roep BO, Stobbe I, Duinkerken G, van Rood JJ, Lernmark A, Keymeulen B, Pipeleers D, Claas FHJ, de Vries RRP.** Auto- and alloimmune reactivity to human islet allografts transplanted into type 1 diabetic patients. *Diabetes* 48: 484–490, 1999.
39. **Sanchez BC, Ochoa-Acuna H, Porterfield DM, Sepulveda MS.** Oxygen flux as an indicator of physiological stress in fathead minnow (*Pimephales promelas*) embryos: a real-time biomonitoring system of water quality. *Environ Sci Technol* 42: 7010–7017, 2008.
40. **Shapiro AM, Lakey JR, Ryan EA, Korbutt GS, Toth E, Warnock GL, Kneteman NM, Rajotte RV.** Islet transplantation in seven patients with type 1 diabetes mellitus using a glucocorticoid-free immunosuppressive regimen. *N Engl J Med* 343: 230–238, 2000.
41. **Siebers U, Horcher A, Bretzel RG, Federlin K, Zekorn T.** Alginate-based microcapsules for immunoprotected islet transplantation. In: *Bioartificial Organs*. New York: NY Acad Sci, 1997, p. 304–312.
42. **Smidsrod O, Skjakbraek G.** Alginate as immobilization matrix for cells. *Trends Biotechnol* 8: 71–78, 1990.
43. **Stull ND, Breite A, McCarthy R, Tersey S, Mirmira R.** Mouse Islet of Langerhans isolation using a combination of purified collagenase and neutral protease. *J Vis Exp* 67: e4137, 2012.
44. **Tersey SA, Nishiki Y, Templin AT, Cabrera SM, Stull ND, Colvin SC, Evans-Molina C, Rickus JL, Maier B, Mirmira RG.** Islet b-cell endoplasmic reticulum stress precedes the onset of type 1 diabetes in the nonobese diabetic mouse model. *Diabetes* 61: 818–827, 2012.
45. **Wang T, Lacik I, Brissova M, Anilkumar AV, Prokop A, Hunkeler D, Green R, Shahrokhi K, Powers AC.** An encapsulation system for the immunoisolation of pancreatic islets. *Nat Biotech* 15: 358–362, 1997.
46. **Wheeler DL, Stokes KE, Hoellrich RG, Chamberland DL, McLoughlin SW.** Effect of bioactive glass particle size on osseous regeneration of cancellous defects. *J Biomed Mater Res* 41: 527–533, 1998.
47. **Xynos ID, Hukkanen MV, Batten JJ, Buttery LD, Hench LL, Polak JM.** Bioglass 45S5 stimulates osteoblast turnover and enhances bone formation In vitro: implications and applications for bone tissue engineering. *Calc Tissue Int* 67: 321–329, 2000.